

# Biodistribution Analysis of Oncolytic Adenoviruses in Canine Patient Necropsy Samples Treated with Cellular Virotherapy

Ana Gómez,<sup>1</sup> David Sardón,<sup>1</sup> Teresa Cejalvo,<sup>2</sup> Fernando Vázquez,<sup>1</sup> Javier García-Castro,<sup>2,3</sup> and Ana Judith Perisé-Barrios<sup>2,3</sup>

<sup>1</sup>Veterinary Pathology Unit, Universidad Alfonso X el Sabio, 28691 Madrid, Spain; <sup>2</sup>Cellular Biotechnology Unit, Instituto de Salud Carlos III, 28220 Madrid, Spain;

<sup>3</sup>Biomedical Research Unit, Universidad Alfonso X el Sabio, 28691 Madrid, Spain

**Oncolytic immunotherapy with competent viruses is an emerging approach in cancer treatment. The clinical safety of many types of oncolytic viruses (OVs) has been demonstrated. However, there is a lack of information about viral biodistribution in patients. The available data about oncolytic adenovirus biodistribution in human subjects treated intravenously consists of virus detection in body fluids, a few tumor biopsies, and a single report of patient necropsy samples. There is no information about adenoviral biodistribution in patients treated intravenously with cellular vehicles carrying an oncolytic adenovirus. We previously published reports regarding the efficacy and clinical safety of infusing mesenchymal stem cells (MSCs) infected with an OV in human and canine patients. In this study, we performed necropsies on 12 canine patients treated with dCelyvir, canine MSCs infected with ICOCAV17, a canine oncolytic adenovirus. The prevalence of microscopic lesions, especially chronic inflammatory responses in different organs, was higher than expected. Concomitantly, we found a positive immunoreaction to ICOCAV17 in analyzed samples. These findings support a possible role of the virus in development of histopathological alterations and ongoing systemic viral replication of ICOCAV17 in the period after therapy administration.**

## INTRODUCTION

Oncolytic viruses (OVs) have emerged as anticancer treatments in human medicine. The US Food and Drug Administration (FDA) and European Medicines Agency (EMA) have recently approved an OV (Imlygic®) as an intratumoral treatment for patients with melanoma.<sup>1</sup> To be able to treat hard-to-reach tumors or disseminated metastases, systemic administration of OVs is necessary. However, most OVs are ineffective when administered intravenously (i.v.) because antiviral immunity, mainly because of neutralizing antiviral antibodies, can hinder systemic virotherapy.<sup>2</sup> In these cases, use of cells with an inherent tumor tropism as vehicles to transport OVs has been suggested to protect them from immune system neutralization and increase the duration of the OVs by evading the antiviral immune response of the patient. This strategy enhances the effectiveness of the

treatment by increasing the number of viral particles released into the tumor.<sup>3,4</sup> For example, use of mesenchymal stem cells (MSCs) that function as a “Trojan horse” delivery vehicle has been proposed.<sup>3</sup> MSCs are multipotent adult stem cells that can self-renew by dividing and can differentiate into multiple tissues, including bone, cartilage, muscle, fat, and connective tissue. These cells are very useful because they possess a high ability to migrate to damaged or inflamed tissues as well as to tumors.<sup>5</sup> MSCs can be infected *in vitro* and injected into patients systemically to home to tumors and release OVs. We developed a strategy called Celyvir for pediatric solid tumors, using human MSCs infected with ICOVIR-5, a human oncolytic adenovirus.<sup>6,7</sup> We reported our initial human clinical results regarding use of Celyvir in patients with advanced neuroblastoma and we described an excellent toxicity profile and several clinical responses, including two complete remissions among 12 patients.<sup>8,9</sup> Similar results were also obtained in a phase I clinical trial for pediatric and adult tumors treated with Celyvir (ClinicalTrials.gov: NCT01844661).<sup>10</sup> Other authors are also using MSCs as antitumoral carriers in human clinical trials against prostate cancer (ClinicalTrials.gov: NCT01983709), ovarian cancer (ClinicalTrials.gov: NCT02530047 and NCT02068794), head and neck cancer (ClinicalTrials.gov: NCT02079324), lung cancer (ClinicalTrials.gov: NCT03298763), and high-grade gliomas (ClinicalTrials.gov: NCT03896568).

Clinical studies conducted in client-owned dogs are very useful for developing new anticancer therapeutic agents<sup>11,12</sup> for human and veterinary medicine. Canine OVs can benefit cancer patients because almost all cancer treatments are palliative, and 50% of dogs older than 10 years diagnosed with cancer die because of tumor progression.<sup>13,14</sup> A human OV based on human Ad5 was generated previously (ICOVIR17), and further promising results were obtained in preclinical studies.<sup>15</sup> Also, a new canine conditionally replicative oncolytic adenovirus (ICOCAV17) based on canine adenovirus serotype

Received 5 April 2020; accepted 10 August 2020;  
<https://doi.org/10.1016/j.omto.2020.08.006>.

**Correspondence:** Ana Judith Perisé Barrios, Biomedical Research Unit, Universidad Alfonso X El Sabio, 28691 Madrid, Spain.

**E-mail:** [aperibar@uax.es](mailto:aperibar@uax.es)



2 (CAV2) containing an tripeptide Arg-Gly-Asp (RGD motif) in the HI loop of the CAV2 fiber was generated. ICOCAV17 possesses similar characteristics as ICOVIR17.

Previously, we published the safety and efficacy of an upgraded canine version of Celyvir (dCelyvir) using dog MSCs (dMSCs) and ICOCAV17.<sup>16</sup> In this study, 27 canine patients with spontaneous sarcomas and central nervous system (CNS) tumors were treated with systemic repeated administration of dCelyvir. Most dogs (59%) received dCelyvir as the only treatment. An excellent toxicity profile was observed, and the clinical response after eight doses of dCelyvir was evaluated using the veterinary response evaluation in solid tumors (RECIST) V1.1 criteria guidelines based on similar human RECIST. Clinical efficacy was observed in 74% of the patients, with 14.8% showing complete remission.<sup>16</sup> Moreover, 2 of 5 canine patients with pulmonary metastases at the moment of diagnosis had a complete response. Secondary effects because of the administration of dCelyvir were rare. None of the patients presented general adverse events, cardiovascular events, or respiratory events. Hematological and biochemical analyses were performed routinely on all patients, showing no alteration in renal, hepatic, or hematological function. There were no significant changes in peripheral blood cell counts. The number of immune cells (i.e., neutrophils, T cells [CD3+, CD4+, and CD8+], macrophages, natural killer cells, and T regulatory cells) in peripheral blood during treatment was analyzed by flow cytometry, and only the increase in T cell number following the first dose was statistically significant. Evaluation of the patients' quality of life revealed that 73% showed a good quality of life during treatment.<sup>16</sup> Patients with a bad quality of life presented osteosarcomas or soft tissue sarcomas affecting the legs, which restricted mobility and caused pain. Despite minimal effects on the overall health of the patients, in the tumors, we observed extracellular matrix alterations and increased immune cell infiltration after treatment with dCelyvir, suggesting activation of the immune system.<sup>16</sup>

Few studies of adenovirus biodistribution have been done in patients using i.v. administered OVs,<sup>17</sup> and there are not much data in patients treated with cellular immunotherapies. Here we wanted to determine the prevalence of histopathological lesions in post-mortem samples taken from dCelyvir-treated dogs that could describe potential histopathological changes of organs and determine adenovirus biodistribution in tissues.

## RESULTS

### Pathological Studies

Systematic necropsies were performed on 12 patients previously diagnosed with sarcomas and treated with dCelyvir. The median number of inoculated dCelyvir doses in dogs was 12.8 (3–28) doses, and the number of days between the last dCelyvir dose and necropsy was 17.08 (2–54) days (Figures 1A and 1B). Most organs exhibited diffuse reddening (perimortem congestion), but apart from the preexisting tumors, no other relevant alterations were observed macroscopically in any analyzed organ.

Histopathological diagnoses of tumors were based on the World Health Organization (WHO) histopathological classification of tumors of domestic animals.<sup>18</sup> Microscopic examination of organs taken from necropsies revealed alterations in several organs (Table 1). There was no correlation between the total number of tissue alterations and the number of days from the last dCelyvir dose to necropsy date or number of doses of dCelyvir received (Figures 1C and 1D). Further, no correlation was observed between the specific tissue with alterations and the number of days from the last dCelyvir dose to necropsy date or number of doses of dCelyvir received (Figures 1E and 1F). However, by taking into account the clinical history of the canine patients, we selected only specific alterations that would be related to dCelyvir treatment, and we graded them (Table 2).

We observed some differences in necropsy samples compared with normal healthy tissues (Figures 2A–2C) and compared with oncologic patient tissues (Figure S1). In the liver, we observed diffuse hepatic degeneration in 11 of 12 dogs (91.7%) and even mild multifocal necrosis in 7 animals (58.3%) (Figure 2D). Seven of them (58.3%) also exhibited chronic diffuse lymphocytic inflammation (Figure 2E). Other findings were the presence of intracellular and intraductal bile pigment (cholestasis) in 50% of animals (Figure 2D, black arrows) and acute multifocal hemorrhages in 7 (58.7%).

Likewise, in the gastrointestinal tract, 10 of 12 dogs (83.3%) exhibited signs of chronic inflammation with moderate diffuse infiltration of the *lamina propria* and submucosa in the small and large intestines (lymphoplasmacytic enteritis) (Figure 2F). Additionally, chronic follicular gastritis was found in 2 dogs (16.6%), and 7 (58.3%) showed diffuse acute catarrhal enteritis (Figure 2G).

Chronic lesions in the kidneys were found frequently. All kidneys from all dogs showed degenerative changes and inflammation in the glomerulus, including membranoproliferative glomerulonephritis (Figure 2H, black arrow), glomerulocystic atrophy (Figure 2H, asterisk), and multifocal degeneration of tubular epithelial cells (Figure 2H, white arrow). Moreover, 50% of the dogs presented multifocal metastatic tubular mineralization in the medulla (Figure 2I, black arrows), and 5 dogs (41.7%) also presented moderate diffuse lymphocytic interstitial nephritis (Figure 2J, black arrow).

Non-specific histopathological alterations were observed in the lungs, liver, pancreas, spleen, and kidneys (Figure 3). The lungs showed anthracosis, interstitial pneumonia, atelectasis, fibrinous bronchopneumonia, edema, and congestion (Figure 3D). The spleens showed multifocal hemosiderosis, siderocalcic plaques, and extramedullary hematopoiesis (Figure 3E). The livers showed cholestasis and congestion because of bile pigment accumulation (Figure 3F). The pancreases showed hemorrhages (Figure 3G), and the kidneys presented glomerular atrophy (Figure 3H).

### Adenovirus Biodistribution

In our previous report, we detected the presence of adenovirus in tumors by immunohistochemistry (IHC).<sup>16</sup> Here the adenovirus

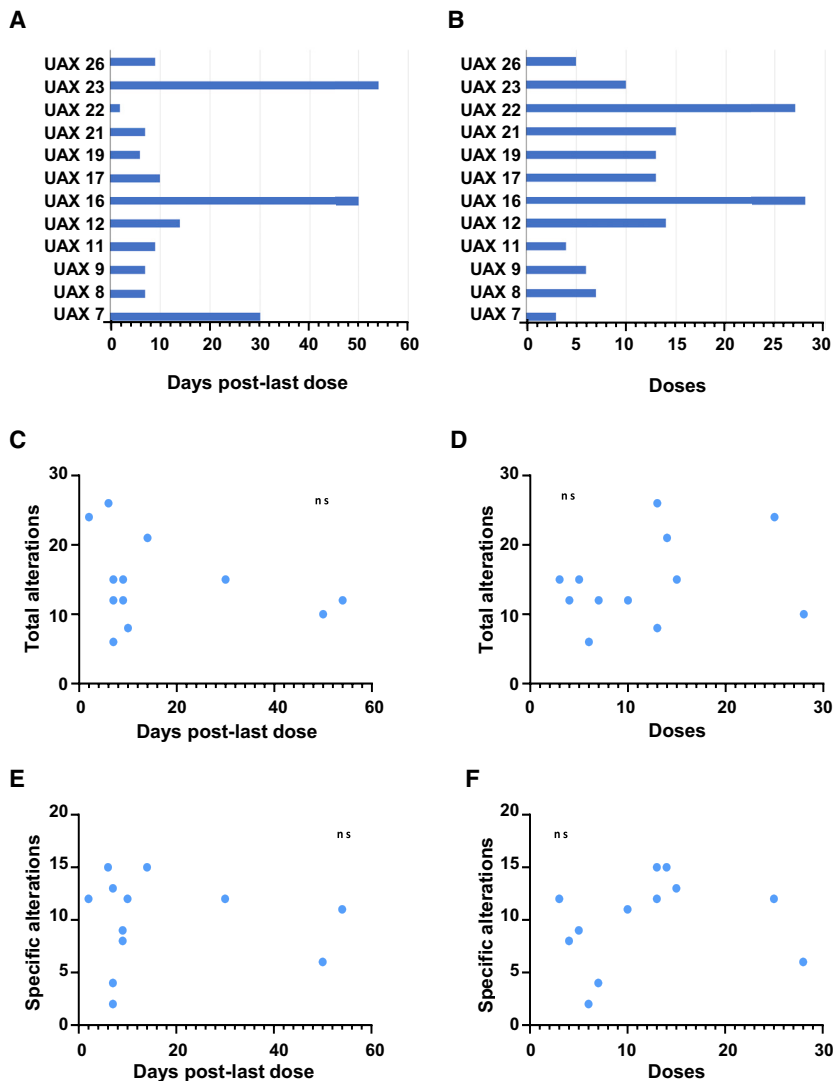


**Figure 1. Significance of Tissue Alterations Found in dCelyvir Patients**

(A) Bars showing the days elapsed from the last dCelyvir dose to necropsy date for each of the patients. (B) Bars showing the number of dCelyvir doses received by each of the patients. (C) Individual patient data (points) showing the total number of tissue alterations and days from the last dCelyvir dose to necropsy. A non-significant (ns) statistical correlation was found between the total number of tissue alterations and the days from the last dCelyvir dose to necropsy date. (D) Individual patient data (points) showing the total number of tissue alterations and doses of dCelyvir received. An ns statistical correlation was found between the total number of tissue alterations and the doses of dCelyvir received. (E) Individual patient data (points) showing the specific tissue alterations and days from the last dCelyvir dose to necropsy. An ns statistical correlation was found between the proposed specific tissue alterations and the days from the last dCelyvir dose to necropsy date. (F) The specific tissue alterations and doses of dCelyvir received by each patient (dots). An ns statistical correlation was found between the proposed specific tissue alterations and the doses of dCelyvir received.

intracellularly. Finally, multiple foci of adenovirus were observed within the primary tumor and metastases (Figure 4F).

## DISCUSSION

In general, most of the side effects described in clinical trials using OV<sub>s</sub> have been common and manageable. The most common side effects were fatigue, nausea/vomiting, chills, and pain, all well-known infection-related symptoms.<sup>19</sup> Our data with Celyvir are similar in human and canine patients, with excellent tolerance of the treatment in most cases, resulting in no clinical secondary effects. However, there is a lack of knowledge about the biodistribution of the vi-

immunostaining detected in other tissues was similar, including positive nuclear, cytoplasmic, and extracellular staining. Positive control tissue (a canine fibrosarcoma intratumorally injected with ICOCV17) showed the same pattern of labeling (Figure 4A). In our pathological analysis, we considered only the presence of focal points of intense and vivid brown color without diffuse spread to be positive.

In general, adenovirus was found multifocally in normal and degenerated ductal epithelial cells of the kidneys (Figure 4B), in epithelial cells of the pancreatic acini (Figure 4C), in hepatocytes (Figure 4D) and in enterocytes (Figure 4E). Interestingly, presence of adenovirus was consistently found to be associated with areas of lymphoplasmacytic infiltration in the digestive tract, liver, and kidneys, in which some of the lymphoid cells (lymphocytes and plasma cells) also expressed the viral protein

ruses after administration in patients. The presence of oncolytic adenoviral DNA was detected in a wide range of tissues in 11 autopsies of human patients enrolled in the Advanced Therapy Access Program at Helsinki University Central Hospital.<sup>17</sup> These patients received their oncolytic adenovirus treatments by ultrasound-guided intratumoral injection, usually combined with an i.v. bolus. The authors reporting this study showed an inverse correlation between the time of the latest virus treatment and the percentage of tissue samples positive for oncolytic adenovirus DNA and the mean virus copy numbers detected in the tissues. Positive samples were detected mainly during the first month post-treatment.<sup>17</sup> In dogs, the wild-type canine adenovirus has affinity for enterocytes, Peyer patches, tubular kidney cells, and hepatocytes,<sup>20,21</sup> and its replication can induce cellular degeneration and necrosis of the infected host cells as well as lymphocytic inflammatory reactions.<sup>22</sup> The severity of microscopic lesions in individual dogs may reflect the duration of

**Table 1. Total Pathological Alterations Found in Necropsies of Dogs Treated with dCelyvir**

Organ	Pathological Alterations	UAX7	UAX8	UAX9	UAX11	UAX12	UAX16	UAX17	UAX19	UAX21	UAX22	UAX23	UAX26
Spleen	hemosiderosis	X	X						X		X		
	lymphocytic depletion										X		
	histiocytosis								X				
	extramedullary hematopoiesis								X		X	X	X
	Gamna-Gandy bodies								X		X		
	thrombosis								X				
	congestion		X					X			X		
Stomach	congestion	X			X				X				
	follicular gastritis		X			X							
Small intestine	mucoïd enteritis	X		X						X			X
	lymphoplasmacytic enteritis	X		X	X	X	X		X	X	X	X	
	congestion	X									X		
	hemorrhages	X											
Large intestine	mucoïd enteritis	X		X						X		X	
	lymphoplasmacytic enteritis	X	X	X	X		X			X	X		X
	congestion	X							X	X			
	hemorrhages		X										
Pancreas	congestion		X		X				X		X	X	X
	hemorrhages		X								X		
Kidney	congestion	X			X	X	X	X	X		X	X	X
	lymphoplasmacytic nephritis					X	X		X			X	X
	membranoproliferative glomerulonephritis		X		X	X	X	X	X	X	X	X	X
	glomerular atrophy			X	X	X	X						
	glomerulosclerosis	X		X	X	X	X	X	X		X	X	X
	metastatic calcification					X	X		X			X	
Liver	congestion	X			X				X				
	edema					X	X	X			X		X
	lymphoplasmacytic hepatitis					X	X		X	X			
	hepatocyte degeneration	X			X	X	X		X	X	X		X
	cholestasis					X	X	X	X		X		X
	hemorrhages		X			X	X	X	X	X	X		
	necrosis	X			X					X			
	thrombosis					X							
Lungs	congestion		X		X			X			X		
	edema		X			X			X		X	X	X
	hemosiderosis					X			X				
	atelectasis					X			X		X		
	anthracosis					X			X				X
	interstitial pneumonia					X			X		X	X	X
	fibrinous bronchopneumonia					X						X	X
	fibrosis								X				
Heart	congestion								X				
	hemorrhages		X			X							

*(Continued on next page)*

**Table 1. Continued**

Organ	Pathological Alterations	UAX7	UAX8	UAX9	UAX11	UAX12	UAX16	UAX17	UAX19	UAX21	UAX22	UAX23	UAX26
Brain	necrosis										X		
	hemorrhages										X		
	astrogliosis										X		
Spinal cord	meningitis						X						

the disease. In the worst cases, fulminant disease is induced by hepatic necrosis and widespread serosal hemorrhage that can affect a variety of organs. The adenovirus infects and replicates in endothelial cells, leading to endothelial cell injury and lysis (necrosis-vasculitis), and this can be followed by hemorrhage and edema and disseminated intravascular coagulation. Large, deeply eosinophilic to amphophilic intranuclear inclusions were found in hepatocytes, vascular endothelium, and Kupffer cells. Inflammation tends to be mild, with lymphocytes and plasma cells being the most abundant cell types.<sup>23</sup> In other report, healthy dogs were treated with conditionally replicative adenoviruses based on CAV2 and transcriptionally targeted to canine osteosarcoma cells. These dogs were inoculated i.v. with  $2 \times 10^{12}$  viral particles (v.p.), and there were no clinical signs of infection and no macroscopic or microscopic changes upon pathological examination 96 h post-inoculation, except mild neutropenia in 3 dogs and severe neutropenia in one dog. Viral DNA was detected at high levels in the spleen and liver.<sup>24</sup> Other authors treated six dogs that had different spontaneous cancers with ICOCV17. Dogs were treated intratumorally with  $1 \times 10^{12}$  v.p. and did not show adverse effects because of the OV. However, toxicity associated with tumor lysis was found in one case, including disseminated intravascular coagulation and systemic failure. In these dogs, viral genomes could be detected in the blood up to a week after treatment, with no viral shedding in the urine, saliva, or feces at any time point.<sup>25</sup>

On dCelyvir, tolerance of treatment was excellent, and clinical adverse events were documented for only 4 of 27 dogs. Two dogs showed mild

skin alterations and one digestion-related symptom, but these were patients that were all concomitantly treated with corticoids. Another patient suffered orchitis. Moreover, few alterations were found in peripheral blood analysis; basically, an increase in alanine transaminase (ALT) levels (grade 1/2) occurred in 10 patients, but only 1 showed concomitantly high aspartate transaminase (AST) levels.<sup>16</sup> In our necropsy anatomopathological analysis, we found unexpected alterations in several organs. These alterations were not as serious as what is seen from wild-type CAV infection, although the absence of changes in the biochemical measurements of peripheral blood contrasts with the involvement seen in some organs of certain dogs. It should be noted that there is no statistical correlation between detected tissue alterations and the number of doses of dCelyvir, when worse damage would be expected in dogs that received a high number of viruses, although the small number of dogs makes this analysis difficult.

Positive anti-adenovirus IHC staining was detected in a wide variety of tissues, indicating the presence of viral proteins in non-tumoral tissues. Our group has shown previously that liver and tumor samples showing positive IHC staining for the canine oncolytic adenovirus were positive for ICOCV17 when analyzed by qPCR using a TaqMan probe, which identified the E1A region. Further, positive results were confirmed by sequencing the products of the qPCR.<sup>16</sup> In this regard, ICOCV17 possesses an insertion of an RGD integrin-binding motif at the fiber knob, which could increase its tropism and infectivity compared with wild-type CAV. In mice, the levels of RGD-modified CAV2 were higher than of CAV2 in the testes, heart, lungs, and kidneys after i.v.

**Table 2. Proposed Specific Pathological Alterations Related to dCelyvir Treatment**

Organ	Pathological Alterations	UAX7	UAX8	UAX9	UAX11	UAX12	UAX16	UAX17	UAX19	UAX21	UAX22	UAX23	UAX26
Small intestine	mucoïd enteritis	2	-	-	-	3	-	-	-	1	2	3	3
	lymphoplasmacytic enteritis	2	-	-	2	-	-	1	2	-	-	-	-
Large intestine	mucoïd enteritis	2	-	-	-	-	-	-	-	1	2	2	1
	lymphoplasmacytic enteritis	2	-	-	-	-	-	1	-	-	-	-	-
Kidney	membranoproliferative glomerulonephritis	-	1	-	1	2	3	2	3	2	3	1	1
	lymphoplasmacytic interstitial nephritis	-	-	-	-	1	-	-	2	-	-	1	1
	glomerulosclerosis	1	-	1	2	2	-	1	1	1	1	1	1
	metastatic calcification	-	3	-	-	1	-	-	1	1	2	1	-
Liver	lymphoplasmacytic hepatitis	-	-	-	-	1	1	2	3	2	-	1	1
	hepatocyte degeneration	3	-	1	3	3	2	3	2	3	2	1	1
	necrosis	-	-	-	-	2	-	2	1	2	-	-	-

Numbers are given based on generic grading criteria. The levels of severity in an ordered list are based on a four-level scale representing absence of lesions (-), mild lesions (1), moderate lesions (2), and severe lesions (3).

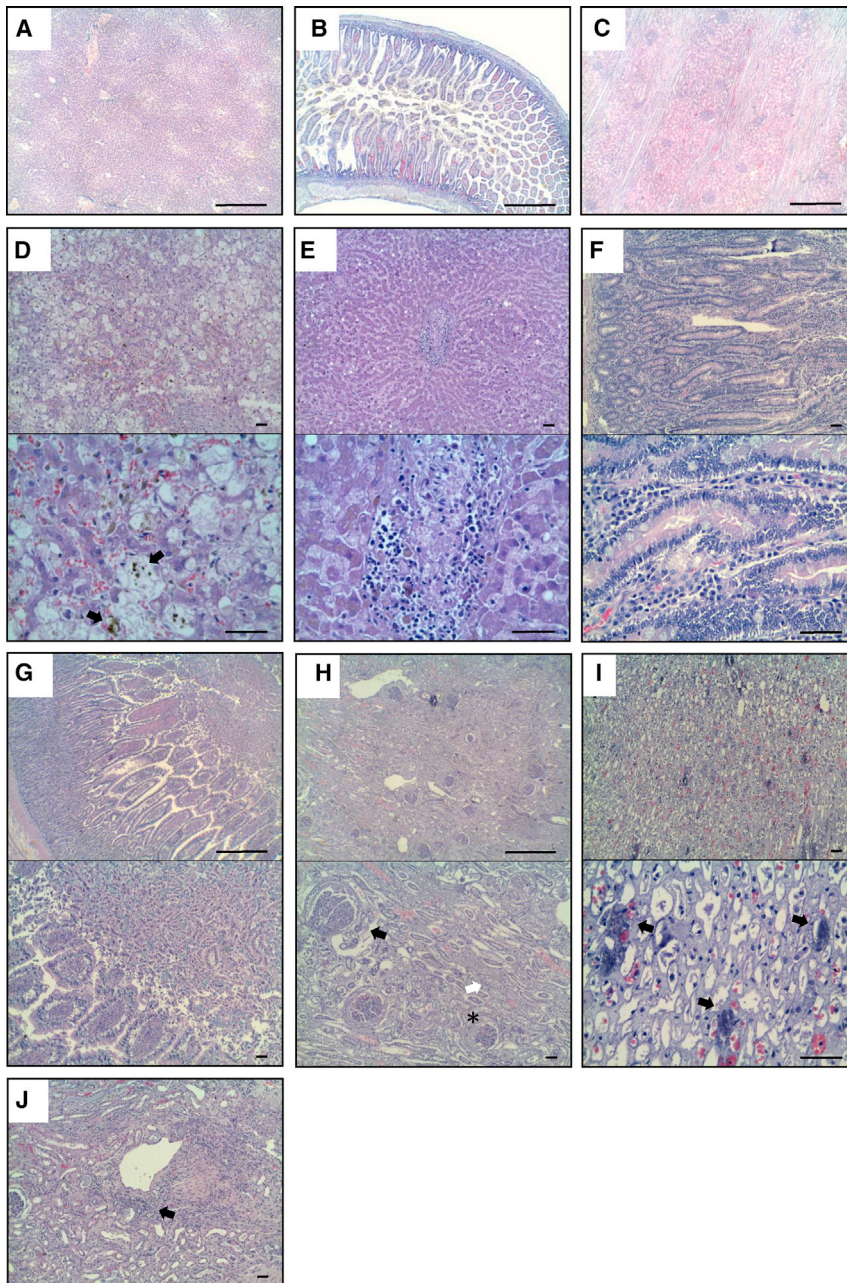


**Figure 2. Alterations Detected in Organs of dCelyvir Patients**

Representative images of hematoxylin and eosin-stained necropsy samples are shown. (A–C) Representative images from healthy dogs: liver (A), gastrointestinal tract (B), and kidney (C) tissues. (D–J) Representative images from dCelyvir-treated dogs. (D and E) Liver showing hepatic degeneration, necrosis (D), and lymphocytic inflammation (E). (F and G) Gastrointestinal tract showing inflammation, lymphoplasmacytic enteritis (F), and catarrhal enteritis (G). (H–J) Kidney samples showing glomerulonephritis (H, black arrow), glomerulocystic atrophy (H, asterisk), degeneration of tubular epithelial cells (H, white arrow), mineralization in the medulla (I, black arrows), and lymphocytic interstitial nephritis (J, black arrow). Scale bars, 1,000  $\mu\text{m}$  (A–C and G and H, top images) and 100  $\mu\text{m}$  (D–F, I, and J and G and H, bottom images). Representative images are shown.

of cell division. Leaky expression of adenoviral genes would also occur following infection of normal quiescent cells, allowing detection of adenoviral proteins.

It is telling that the adenovirus was consistently found to be associated with areas of lymphoplasmacytic infiltration, suggesting an immune reaction against the adenovirus. Surprisingly, the immune system is not able to eliminate the virus. The adenovirus elicits strong innate inflammatory responses within hours after administration, including production of neutralizing antibodies to viral capsid proteins (fiber, hexon, penton).<sup>26</sup> Moreover, CAV vaccines in dogs are quite common (8 of 12 of our patients), and in our study we reported the presence of antibodies against CAV2 prior to dCelyvir treatment, which subsequently increased and stabilized at higher levels after the second dose. Interestingly, these high levels of anti-CAV antibodies did not prevent the antitumoral effects of dCelyvir.<sup>16</sup>

We propose the hypothesis that subclinical and sustained systemic inflammation may be part of the antitumoral mechanism of action of Celyvir therapy, partially mediated by the immune system, including

release of pro-inflammatory cytokines, chemokines, and other danger signals. In summary, our results strongly encourage continued use of a comparative analysis between dogs and humans with the aim of improving immunotherapies based on OVs.

## MATERIALS AND METHODS

### Clinical Study

Data from our veterinary clinical study were published previously.<sup>16</sup> Briefly, 27 canine patients were treated with dCelyvir. The clinical

inoculation.<sup>25</sup> On the other hand, in ICOCV17, E2F-binding sites were inserted in the endogenous E1a promoter, and the pRb (retinoblastoma protein)-binding site of E1a was deleted. Thus, to initiate adenoviral replication, it is necessary to release cellular E2F from pRb-E2F complexes. During G0 and early G1 of the cell cycle, Rb (retinoblastoma) physically associates with E2F factors and blocks their transactivation domain. In late G1, phosphorylated Rb releases E2F, allowing expression of genes that encode products necessary for S phase progression.<sup>26</sup> Therefore, ICOCV17 would initiate its viral cycle in normal cells by taking advantage of E2F release during these phases

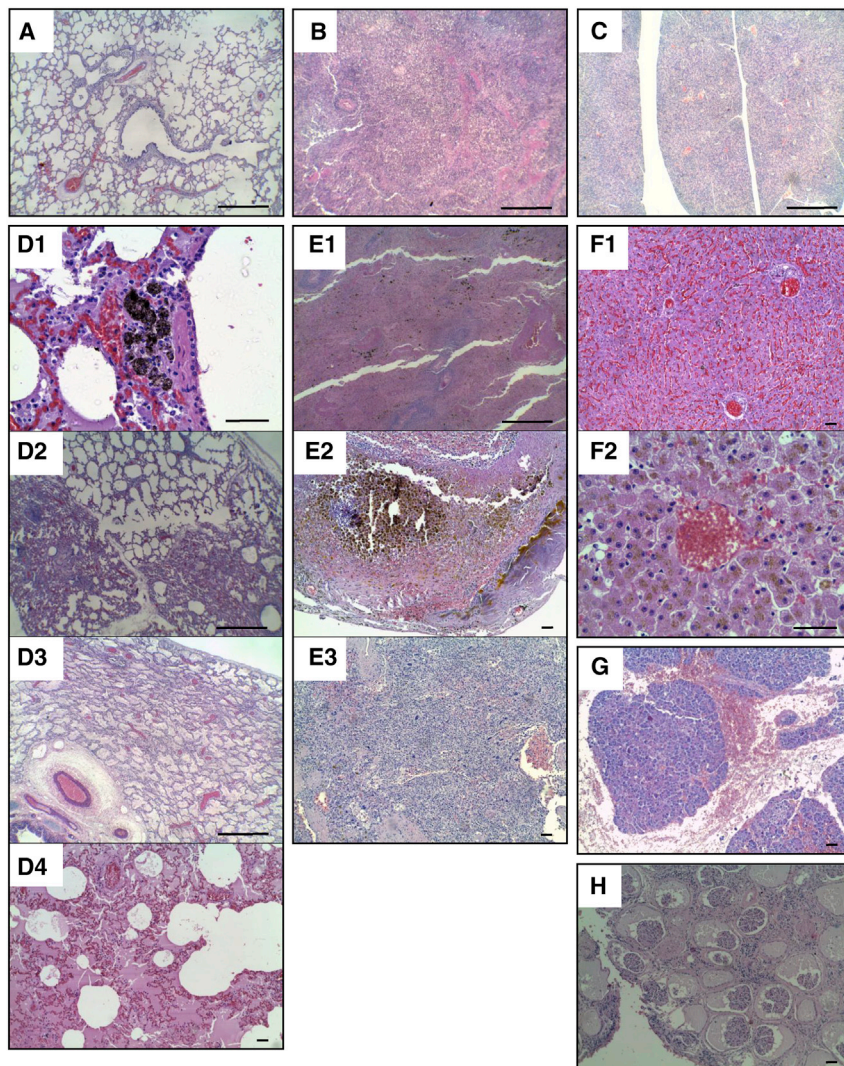


**Figure 3. The Most Prevalent Non-specific Histopathological Alterations Detected in Organs of dCelyvir Patients**

Representative images of hematoxylin and eosin-stained necropsy samples are shown. (A–C) Representative images from healthy dogs: lung (A), spleen (B), and pancreas (C) tissues. (D–H) Representative images from dCelyvir-treated dogs. (D) Lung showing anthracosis (D<sub>1</sub>), interstitial pneumonia and atelectasis (D<sub>2</sub>), fibrinous bronchopneumonia (D<sub>3</sub>), edema (D<sub>4</sub>), and congestion (D<sub>3</sub> and D<sub>4</sub>). (E) Spleen showing multifocal hemosiderosis (E<sub>1</sub>), Gamma-Gandy bodies (siderocalcic plaques; E<sub>2</sub>), and extramedullary hematopoiesis (E<sub>3</sub>). (F) Liver showing congestion (F<sub>1</sub>) and cholestasis (bile pigment accumulation; F<sub>2</sub>). (G) Pancreas showing hemorrhages. (H) Kidney exhibiting multifocal glomerular atrophy. Scale bars, 1,000  $\mu\text{m}$  (A–C, D<sub>2</sub>, D<sub>3</sub>, and E<sub>1</sub>) and 100  $\mu\text{m}$  (D<sub>1</sub>, D<sub>4</sub>, E<sub>2</sub>, E<sub>3</sub>, and F–H). Representative images are shown.

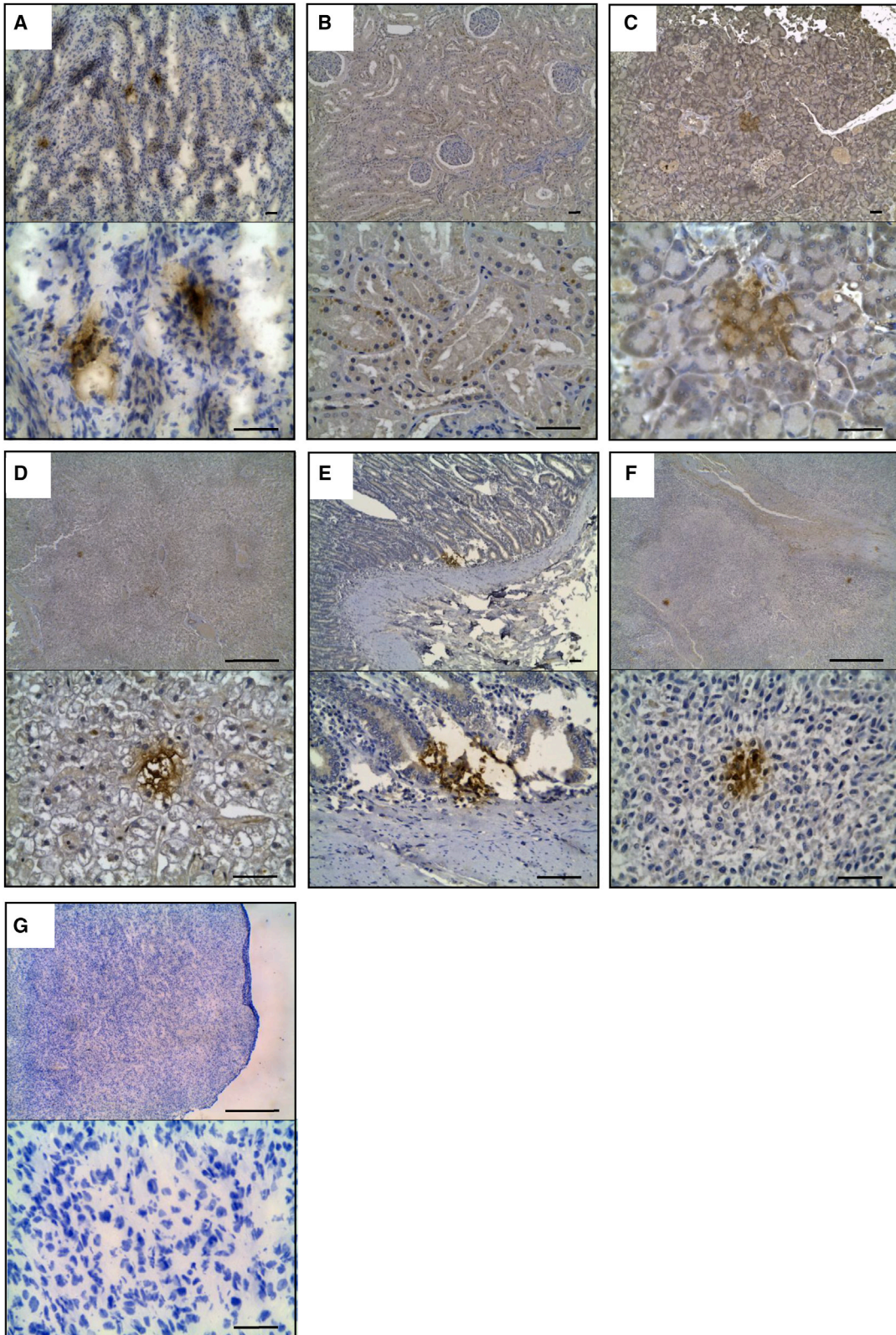
weekly administrations of i.v. dCelyvir ( $0.5 \times 10^6$  cells/kg). Prior to dCelyvir infusion, canine patients were treated i.v. with methylprednisolone (1 mg/kg), metamizole (30 mg/kg), and diphenhydramine (0.5 mg/kg). dCelyvir was administered over 45 min through a peripheral or central venous line (preferably cephalic/saphenous). During the first administration, patients were kept in the hospital for 6 h with constant monitoring. Treatment was repeated once a week for 4 weeks. This treatment cycle was repeated up to a maximum of 7 cycles (28 doses), depending on the patient's clinical response.

The adenovirus used for dMSC infection was ICOCAV17. This OV is based on CAV2, the canine wild-type virus serotype 2, with an RGD motif inserted into the HI loop of the CAV2 fiber. ICOCAV17 is a conditionally replicative adenovirus

in which the endogenous E1a promoter has been modified by inserting four palindromic E2F-binding sites and one Sp-I-binding site. Moreover, 21 base pairs from the E1a pRB-binding domain (E1a $\Delta$ 21) (homologous to  $\Delta$ 24 in human oncolytic adenoviruses) have been deleted. ICOCAV17 is also armed with the human PH20 hyaluronidase (PH20) gene inserted after the fiber under control of the canine IIIa protein splicing acceptor (IIIaSA).<sup>25</sup>

study was approved by the Veterinary Hospital Ethics Committee, and all patient owners gave written informed consent. Inclusion criteria were owner acceptance, disease progression during standard treatment (chemotherapy/surgery), absence of severe underlying disease, and docile character for easy treatment without sedation. The study included several dog breeds. dMSCs were obtained from adipose tissue from healthy donors by mechanically disaggregating the tissue and incubating with type IV collagenase for 45 minutes at 37°C. Cells were filtered through a 70- $\mu\text{m}$  nylon mesh cell strainer and washed with phosphate-buffered saline. Cells were seeded at 10,000 cells/cm<sup>2</sup> with DMEM, supplemented with 10% fetal bovine serum (FBS), 1% glutamine, streptomycin (100 mg/mL) and penicillin (100 U/mL) at 37°C in a humidified atmosphere with 5% CO<sub>2</sub>. For treatment with dCelyvir, dMSCs were infected with ICOCAV17 at a multiplicity of infection (MOI) of 1 infectious particle per cell during 1 h. Infected cells were washed three times, filtered, and resuspended in saline buffer. The study consisted of repeated

The dogs analyzed in the present study presented different clinical responses. Four of the 12 analyzed dogs (UAX8, UAX9, UAX11, and UAX26) presented progressive disease (PD), seven achieved stabilization of disease (SD), and one (UAX23) presented complete remission (CR) following RECISt.<sup>16</sup> Some animals died naturally and others were sacrificed following humanitarian criteria. The moment of sacrificing an animal was decided by criteria of the code of ethics for the practice of veterinary medicine in Spain (COL-VET 2018).



(legend on next page)



## Histopathology

Systematic necropsies were performed on 12 patients, and samples were taken from different organs (spleen, stomach, small and large intestine, pancreas, kidneys, liver, lungs, heart, brain, and spinal cord), fixed in 10% neutral buffered formalin for 48 h, and paraffin wax embedded for histopathology and IHC.

The alterations of tissues were graded semiquantitatively according to degeneration parameters. The following scale was considered: grade 0, absence of degeneration; grade 1, mild; grade 2, moderate; grade 3, intense degeneration.

## IHC

We previously report the specificity of this IHC analyzing the positive tissues for adenovirus by qPCR method.<sup>16</sup> Briefly, for qPCR using formalin-fixed, paraffin-embedded tissues, DNA was extracted from 6 sections of 10  $\mu\text{m}$  and was processed using the Cobas DNA Sample Preparation Kit (Roche). DNA quantification and purity (A260/280 and A260/230) were analyzed with a Nanodrop 2000 spectrophotometer. qPCR products were treated with ExoSAP-IT (ThermoFisher) and were sequenced with primer at 0.6  $\mu\text{mol/L}$  using the capillary automatic sequencer DNA Analyzer 3730xl (Applied Biosystems). Sequences resulting from the sequencing process were analyzed with the Basic Local Alignment Search Tool (BLAST) from the NCBI, and those that produced significant alignments were considered to be positive results.<sup>16</sup> To analyze the presence of ICOCV17 in organs, samples from 12 patients were processed for immunostaining. ICOCV17 immunolabeling was performed on dewaxed sections with the streptavidin-biotin-complex peroxidase method after a high-temperature antigen unmasking procedure and endogenous peroxidase inhibition. The slides were first incubated with normal horse serum (R.T.U.-Vectastain kit). The primary antibody used was polyclonal rabbit anti-human adenovirus 5 antibody (Abcam), which recognizes proteins of the capsid (hexon, penton, etc.) but also protein V, VI, VII, and IX of type 5 adenovirus (overnight incubation at 4°C). The slides were subsequently incubated with biotinylated universal secondary antibody R.T.U. horse anti-mouse/rabbit immunoglobulin G (IgG) (H+L) (R.T.U.-Vectastain Kit) for 1 h at room temperature, followed by incubation with streptavidin conjugated to peroxidase (10 min at room temperature). For all washes and dilutions, Tris-buffered saline (TBS) (pH 7.4) was used. The immune reaction was developed with a chromogen solution containing 3-3' diaminobenzidine tetrachloride and  $\text{H}_2\text{O}_2$  in TBS. Finally, the slides were counterstained with hematoxylin. A sample from a sarcoma-growing in an immunodeficient mouse- that had been intratumorally injected with ICOCV17 was used as a positive control following the protocol described above and as a negative control without using primary antibody.

## Statistical Analysis

Data were analyzed and graphed with GraphPad Prism (GraphPad). Significant differences were determined using paired or non-paired non-parametric tests (Pearson and Spearman test, respectively).  $p < 0.05$  was considered to be statistically significant.

## SUPPLEMENTAL INFORMATION

Supplemental Information can be found online at <https://doi.org/10.1016/j.omto.2020.08.006>.

## AUTHOR CONTRIBUTIONS

A.G., D.S., and T.C. conducted the experiments. D.S., F.V., J.G.-C., and A.J.P.-B. analyzed data. J.G.-C. and A.J.P.-B. designed the experiments, wrote the paper and supervised the project.

## CONFLICTS OF INTEREST

The authors declare no competing financial interests. The content is solely the responsibility of the authors and does not necessarily represent the official views of the ISCIII or the UAX.

## ACKNOWLEDGMENTS

The authors would like to thank Paloma Rey Porto for technical support. ICOCV17 was kindly provided by Dr. Ramón Alemany Bonastre (IDIBELL-Institut Català d'Oncologia, l'Hospitalet de Llobregat). This study was funded by Fundación Universidad Alfonso X el Sabio, Madrid, Spain (1.010.909 to A.J.P.-B.); Instituto de Salud Carlos III, Spain (PI14CIII/00005 and PI17CIII/00013 to J.G.-C.); Consejería de Educación, Juventud y Deporte, Comunidad de Madrid, Spain (P2017/BMD-3692 to J.G.-C.); Fundación Oncohematología Infantil; AFANION; and Asociación Pablo Ugarte, whose support we gratefully acknowledge. The graphical abstract was created with BioRender.

## REFERENCES

1. Kaufman, H.L., Kohlhapp, F.J., and Zloza, A. (2015). Oncolytic viruses: a new class of immunotherapy drugs. *Nat. Rev. Drug Discov.* *14*, 642–662.
2. Ong, H.T., Hasegawa, K., Dietz, A.B., Russell, S.J., and Peng, K.-W. (2007). Evaluation of T cells as carriers for systemic measles virotherapy in the presence of antiviral antibodies. *Gene Ther.* *14*, 324–333.
3. Power, A.T., and Bell, J.C. (2008). Taming the Trojan horse: optimizing dynamic carrier cell/oncolytic virus systems for cancer biotherapy. *Gene Ther.* *15*, 772–779.
4. Chute, J.P. (2006). Stem cell homing. *Curr. Opin. Hematol.* *13*, 399–406.
5. Ramírez, M., García-Castro, J., Melen, G.J., González-Murillo, Á., and Franco-Luzón, L. (2015). Patient-derived mesenchymal stem cells as delivery vehicles for oncolytic virotherapy: novel state-of-the-art technology. *Oncolytic Virother.* *4*, 149–155.
6. Ramírez, M., García-Castro, J., and Alemany, R. (2010). Oncolytic virotherapy for neuroblastoma. *Discov. Med.* *10*, 387–393.
7. Cascallo, M., Alonso, M.M., Rojas, J.J., Perez-Gimenez, A., Fueyo, J., and Alemany, R. (2007). Systemic toxicity-efficacy profile of ICOCV-5, a potent and selective oncolytic adenovirus based on the pRB pathway. *Mol. Ther.* *15*, 1607–1615.

## Figure 4. Adenovirus Detected by IHC in Organs of dCelyvir Patients

(A) Canine fibrosarcoma infected intratumorally with ICOCV17 as positive control. (B–F) Images showing adenovirus-positive cells in the kidneys (B), pancreas (C and D), enterocytes (E), and tumor and metastasis (F) Formalin-Fixed Paraffin-Embedded (FFPE) samples. (G) IHC without primary antibody in canine fibrosarcoma infected intratumorally with ICOCV17 as negative control. Scale bars, 100  $\mu\text{m}$  (A–C and E and D, F, and G, bottom images) and 1000  $\mu\text{m}$  (D, F, and G top images). Representative images are shown.

8. García-Castro, J., Alemany, R., Cascalló, M., Martínez-Quintanilla, J., Arriero, Mdel.M., Lassaletta, A., Madero, L., and Ramírez, M. (2010). Treatment of metastatic neuroblastoma with systemic oncolytic virotherapy delivered by autologous mesenchymal stem cells: an exploratory study. *Cancer Gene Ther.* 17, 476–483.
9. Melen, G.J., Franco-Luzón, L., Ruano, D., González-Murillo, Á., Alfranca, A., Casco, F., Lassaletta, Á., Alonso, M., Madero, L., Alemany, R., et al. (2016). Influence of carrier cells on the clinical outcome of children with neuroblastoma treated with high dose of oncolytic adenovirus delivered in mesenchymal stem cells. *Cancer Lett.* 371, 161–170.
10. Ramirez, M., Ruano, D., Moreno, L., Lassaletta, Á., Bautista, F.J., Andión, M., et al. (2018). First-in-child trial of Celyvir (Autologous mesenchymal stem cells carrying the oncolytic virus ICOVIR-5) in patients with relapsed and refractory pediatric solid tumors. *J. Clin. Oncol.* 36, 10543.
11. Paoloni, M., and Khanna, C. (2008). Translation of new cancer treatments from pet dogs to humans. *Nat. Rev. Cancer* 8, 147–156.
12. Kol, A., Arzi, B., Athanasiou, K.A., Farmer, D.L., Nolte, J.A., Rebhun, R.B., Chen, X., Griffiths, L.G., Verstraete, F.J., Murphy, C.J., and Borjesson, D.L. (2015). Companion animals: Translational scientist's new best friends. *Sci. Transl. Med.* 7, 308ps21.
13. Patil, S.S., Gentschev, I., Nolte, I., Ogilvie, G., and Szalay, A.A. (2012). Oncolytic virotherapy in veterinary medicine: current status and future prospects for canine patients. *J. Transl. Med.* 10, 3.
14. Hansen, K., and Khanna, C. (2004). Spontaneous and genetically engineered animal models; use in preclinical cancer drug development. *Eur. J. Cancer* 40, 858–880.
15. Guedan, S., Rojas, J.J., Gros, A., Mercade, E., Cascallo, M., and Alemany, R. (2010). Hyaluronidase expression by an oncolytic adenovirus enhances its intratumoral spread and suppresses tumor growth. *Mol. Ther.* 18, 1275–1283.
16. Cejalvo, T., Perisé-Barrios, A.J., Del Portillo, I., Laborda, E., Rodríguez-Milla, M.A., Cubillo, I., Vázquez, F., Sardón, D., Ramirez, M., Alemany, R., et al. (2018). Remission of Spontaneous Canine Tumors after Systemic Cellular Viroimmunotherapy. *Cancer Res.* 78, 4891–4901.
17. Koski, A., Bramante, S., Kipar, A., Oksanen, M., Juhila, J., Vassilev, L., Joensuu, T., Kanerva, A., and Hemminki, A. (2015). Biodistribution Analysis of Oncolytic Adenoviruses in Patient Autopsy Samples Reveals Vascular Transduction of Noninjected Tumors and Tissues. *Mol. Ther.* 23, 1641–1652.
18. Beveridge, W.I., and Sobin, L.H. (1976). International histological classification of tumours of domestic animals: Introduction. *Bull. World Health Organ.* 53, 137–141.
19. Matsuda, T., Karube, H., and Aruga, A. (2018). A Comparative Safety Profile Assessment of Oncolytic Virus Therapy Based on Clinical Trials. *Ther. Innov. Regul. Sci.* 52, 430–437.
20. Patil, S.S., Gentschev, I., Adelfinger, M., Donat, U., Hess, M., Weibel, S., Nolte, I., Frentzen, A., and Szalay, A.A. (2012). Virotherapy of canine tumors with oncolytic vaccinia virus GLV-1h109 expressing an anti-VEGF single-chain antibody. *PLoS ONE* 7, e47472.
21. Greene, C.E. (2012). In *Infectious diseases of the dog and cat*, Fourth Edition (Elsevier), p. 1354.
22. Decaro, N., Martella, V., and Buonavoglia, C. (2008). Canine Adenoviruses and Herpesvirus. *Vet. Clin. North Am. Small Anim. Pract.* 38, 799–814.
23. Maxie, M.G. (2015). Infectious diseases of the respiratory system. In *Jubb, Kennedy, and Palmer's pathology of domestic animals*, Sixth Edition (Elsevier).
24. Smith, B.F., Curiel, D.T., Ternovoi, V.V., Borovjagin, A.V., Baker, H.J., Cox, N., and Siegal, G.P. (2006). Administration of a conditionally replicative oncolytic canine adenovirus in normal dogs. *Cancer Biother. Radiopharm.* 21, 601–606.
25. Laborda, E., Puig-Saus, C., Rodríguez-García, A., Moreno, R., Cascalló, M., Pastor, J., and Alemany, R. (2014). A pRb-responsive, RGD-modified, and hyaluronidase-armed canine oncolytic adenovirus for application in veterinary oncology. *Mol. Ther.* 22, 986–998.
26. Giacinti, C., and Giordano, A. (2006). RB and cell cycle progression. *Oncogene* 25, 5220–5227.

**OMTO, Volume 18**

## **Supplemental Information**

### **Biodistribution Analysis of Oncolytic**

### **Adenoviruses in Canine Patient Necropsy**

### **Samples Treated with Cellular Virotherapy**

**Ana Gómez, David Sardón, Teresa Cejalvo, Fernando Vázquez, Javier García-Castro, and Ana Judith Perisé-Barrios**

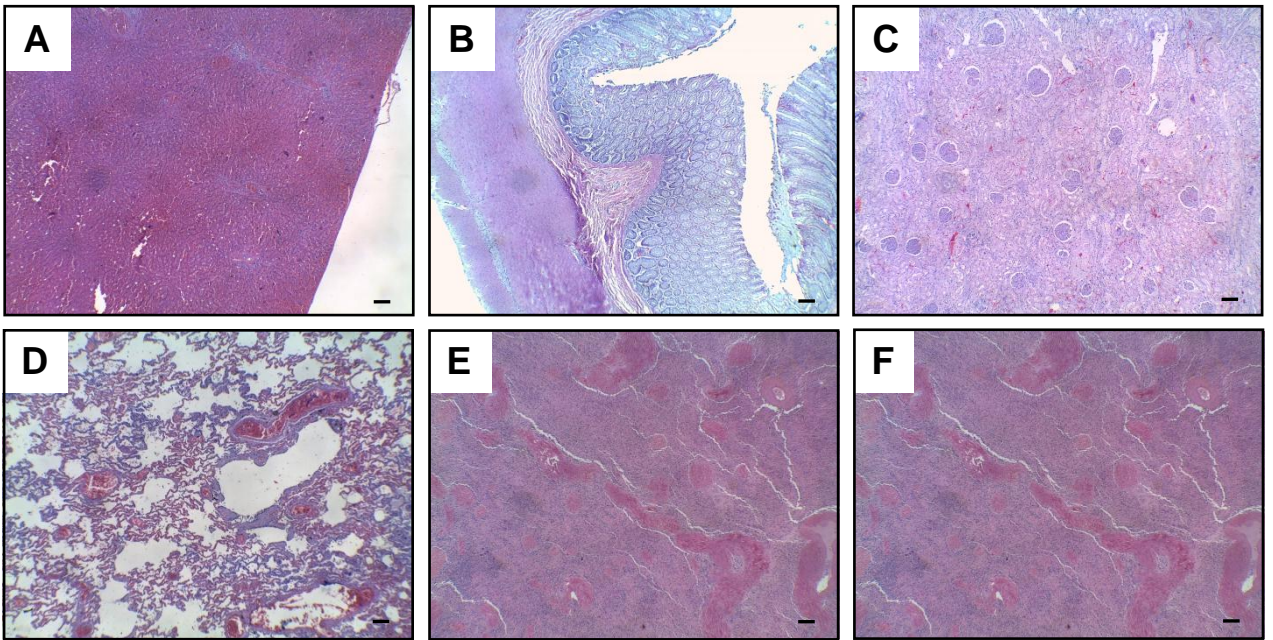


**Figure S1. Tissues from oncologic patients treated with conventional treatment are shown.** Representative images of hematoxylin and eosin stained necropsy samples from liver (A), gastrointestinal tract (B), kidney (C), lung (D), spleen (E) and pancreas (F) are shown. Scale bar: 100  $\mu$ m.